

# Experimental Method to Constrain Preferential Emission and Spectator Dynamics in Heavy-Ion Collisions

Somadutta Bhatta<sup>a,\*</sup>, Vipul Bairathi<sup>b,\*\*</sup>

<sup>a</sup>*Department of Chemistry, Stony Brook University, Stony Brook, 11794, New York, USA*

<sup>b</sup>*Instituto de Alta Investigación, Universidad de Tarapacá, Casilla 7D, Arica, 1000000, Chile*

---

## Abstract

We present the first experimental method to directly correlate initial participant asymmetry with final-state multiplicity to quantify contribution of preferential emission to the rapidity-odd component of pseudorapidity distribution of produced particles in heavy-ion collisions. Within a transport model simulation, the correlator displays an increase from mid to large rapidities and from central to peripheral collisions. It also displays sensitivity to spectator dynamics, with its magnitude decreasing as more spectators undergo evaporation or fragmentation. The proposed correlator provides a powerful experimental tool to constrain particle production mechanisms and the space-time evolution of spectator matter in heavy-ion collisions.

*Keywords:* Particle Production, Preferential Emission, Spectator Dynamics

*PACS:* 25.75.Dw; 25.75.Gz

---

**Introduction.** Understanding the mechanisms of particle production is one of the primary goals in high-energy heavy-ion collisions. In particular, understanding the nature of particle production governing the pseudorapidity ( $\eta$ ) distribution is essential for constraining the three-dimensional profile of energy and entropy density in the initial state. [1–6]. Significant progress in this direction has been made through experimental measurements and phenomenological investigations on forward-backward multiplicity-correlations, flow-decorrelations, and baryon-stopping [7–13].

In QCD-inspired string models like HIJING and AMPT, particle production occurs through string formation, where the number of strings is equal to the number of participant nucleons ( $N_{\text{part}}$ ) [14, 15]. Color-neutral hadrons are produced through string breaking. Event-by-event fluctuations in string lengths and endpoints lead to variations in the longitudinal distribution of produced particles,  $P(\eta)$  [15–18]. Previous studies of forward-backward multiplicity correlations and  $P(\eta)$  in asymmetric collision systems suggest that nucleons emit more particles in the direction of their motion, with forward (backward) moving nucleons emitting more particles in forward (backward)  $\eta$  [13, 19–21]. This behavior, known as preferential emission, and the forward-backward asymmetry of  $N_{\text{part}}$ , results in event-by-event asymmetry in  $P(\eta)$  as well as long-range multiplicity correlations in  $\eta$  [11]. Moreover, the preferential emission mechanism is crucial for explaining longitudinal flow-decorrelations and directed-flow [7, 22–25]. Therefore, developing novel observables that capture the correlation between the forward-backward asymmetry of  $N_{\text{part}}$  and multiplicity in experimental measurements is crucial to provide stronger constraints on the mechanism of preferential emission.

In heavy-ion collision experiments,  $N_{\text{part}}$  cannot be directly measured; however, neutron and proton spectators can be detected by the Zero-Degree Calorimeters (ZDC) and Forward Proton Detectors (AFP) [26–29]. But again, not all spectators are detected experimentally due to dynamic processes such as fragmentation and evaporation. The Abrasion-Ablation model [30, 31] describes this process: participant nucleons are sheared from the colliding nuclei (Abrasion), exciting the spectator fragment, which then de-excites through

---

\*Corresponding Author

\*\*Corresponding Author

*Email addresses:* somadutta.bhatta@stonybrook.edu (Somadutta Bhatta), vipul.bairathi@gmail.com (Vipul Bairathi)

multi-fragmentation or evaporation (Ablation). These processes produce charged fragments that deviate from the expected trajectories of spectator nucleons due to differences in charge-to-mass ratios, resulting in a loss of detectable spectators. Since the separation of spectators from participants during collisions involves energy exchange between nucleons, and the subsequent dynamics depend on nuclear energy levels, constraining this process is crucial for understanding fundamental aspects of nucleon emission mechanism and the Equation of State (EoS) of nuclear matter [32–35].

Currently, experimental measurements rely on model comparisons to understand the contribution of  $N_{\text{part}}$  asymmetry towards rapidity-odd component of  $P(\eta)$ . A key feature of this study is to correlate  $N_{\text{part}}$  asymmetry with final-state multiplicity asymmetry to directly quantify this contribution. Moreover, the modeling of spectator dynamics in heavy-ion collisions is inadequate, particularly for observables at lower collision energies where spectator dynamics are expected to play a significant role [36–38]. The proposed correlator in this study also aims to capture the fluctuations in number of spectators due to fragmentation and evaporation, providing stronger constraints on modeling these dynamic processes.

**Method.** In heavy-ion collisions, nucleons that undergo collisions are called “participants”, while those moving along the beam direction without interacting are called “spectators”. The total  $N_{\text{part}}$  is the sum of forward ( $N_{\text{part,F}}$ ) and backward ( $N_{\text{part,B}}$ ) moving participants, which fluctuate event-by-event due to quantum mechanical effects. Previous studies [39, 40] indicate that the initial asymmetry between  $N_{\text{part,F}}$  and  $N_{\text{part,B}}$  in an event contributes asymmetrically to  $P(\eta)$  around  $\eta = 0$  [19, 22, 41–43]. The contribution of this asymmetry can be quantified by correlating the forward-backward asymmetry of participants in the initial state with the forward-backward asymmetry of produced particles in the final state on an event-by-event basis.

In the past, preferential emission has been studied within models that include the fragmentation of wounded nucleons [13, 19–21]. Similar features have also been reported in the A Multi-Phase Transport (AMPT) model [11, 44]. The AMPT model, widely used to simulate the space-time evolution of matter formed in heavy-ion collisions, provides a good description of experimentally measured collective-flow and particle spectra [45–52]. Therefore, this study utilizes the AMPT model to simulate Au+Au collisions at  $\sqrt{s_{NN}} = 200$  GeV. The total number of pions, kaons, and protons with transverse momentum  $p_T < 10$  GeV constitutes the multiplicity ( $N_{\text{ch}}$ ) in an event. Centrality is determined by dividing the distribution of  $N_{\text{ch}}$  within  $|\eta| < 0.2$  into percentiles, where centrality of 0% corresponds to the most central collisions with largest  $N_{\text{ch}}$ . All observables in this study are calculated for  $|\eta| > 0.2$  to avoid any overlap between the  $N_{\text{ch}}$  used for determining centrality and those used for calculating the observables.

Motivated by previous studies [19, 22, 41–43], we begin with the general idea that  $P(\eta)$  has contributions from both rapidity-odd and rapidity-even sources of particle production, with the rapidity-even components contributing symmetrically about  $\eta = 0$ . The forward-backward multiplicity asymmetry in each event can be defined as:  $A_{\text{ch},\eta} = N_{\text{ch},\eta} - N_{\text{ch},-\eta}$ , where  $N_{\text{ch},\eta}$  is the number of charged particles within a narrow interval  $\delta\eta$ , centered at  $\eta$ . The  $A_{\text{ch},\eta}$  is an odd function of  $\eta$ , as  $A_{\text{ch},\eta} = -A_{\text{ch},-\eta}$ , capturing the rapidity odd-component. Similarly, the participant asymmetry in each event is defined as:  $A_{\text{part}} = N_{\text{part,F}} - N_{\text{part,B}}$ . The number of forward-going spectators,  $N_{\text{spec,F}}$  is anti-correlated to  $N_{\text{part,F}}$ , as  $N_{\text{spec,F}} = A - N_{\text{part,F}}$ , where  $A$  is the nucleus’s mass number. So,  $A_{\text{part}} = -A_{\text{sp}} = N_{\text{spec,B}} - N_{\text{spec,F}}$ , where  $A_{\text{sp}}$  is the asymmetry between forward and backward moving spectators. By correlating  $A_{\text{ch},\eta}$  with  $A_{\text{sp}}$  on an event-by-event basis, we can quantify the contribution of initial-state participant asymmetry to the rapidity-odd component of the longitudinal distribution of produced particles.

To reduce the effect of efficiency and resolution of spectator detection using ZDC and AFP in experiments [26, 27, 53], the asymmetry variables are normalized as follows:

$$nA_{\text{sp}} = \frac{N_{\text{spec,F}} - N_{\text{spec,B}}}{N_{\text{spec,F}} + N_{\text{spec,B}}}, \quad nA_{\text{ch},\eta} = \frac{N_{\text{ch},\eta} - N_{\text{ch},-\eta}}{N_{\text{ch},\eta} + N_{\text{ch},-\eta}}. \quad (1)$$

Finally,  $nA_{\text{sp}}$  is correlated with  $nA_{\text{ch},\eta}$  using Pearson correlation coefficient following:

$$\rho(nA_{\text{sp}}, nA_{\text{ch},\eta}) = -\frac{\text{Cov}(nA_{\text{sp}}, nA_{\text{ch},\eta})}{\sqrt{\text{Var}(nA_{\text{sp}})\text{Var}(nA_{\text{ch},\eta})}}, \quad (2)$$

where, covariance between  $nA_{\text{sp}}$  and  $nA_{\text{ch},\eta}$  is given by  $Cov(nA_{\text{sp}}, nA_{\text{ch},\eta})$ , and their variances are given by,  $Var(nA_{\text{sp}})$  and  $Var(nA_{\text{ch},\eta})$ . The distributions for  $nA_{\text{sp}}$  and  $nA_{\text{ch},\eta}$  over many events have a mean of 0, implying  $Cov(nA_{\text{sp}}, nA_{\text{ch},\eta}) = \langle nA_{\text{sp}} \cdot nA_{\text{ch},\eta} \rangle$ , and  $Var(nA_{\text{sp}}) = \langle (nA_{\text{sp}})^2 \rangle$ , where,  $\langle \rangle$  denotes averaging over an event ensemble. The negative sign used in Eq. 2 converts spectator asymmetry to participant asymmetry,  $nA_{\text{part}}$ , where, for a fixed  $N_{\text{part}}$ ,

$$nA_{\text{part}} = \frac{N_{\text{part},\text{F}} - N_{\text{part},\text{B}}}{N_{\text{part},\text{F}} + N_{\text{part},\text{B}}}, nA_{\text{sp}} = -\frac{N_{\text{part}}}{N_{\text{spec}}} nA_{\text{part}}. \quad (3)$$

The losses in number of spectators in forward and backward directions owing to spectator dynamics does not affect particle production near mid-rapidity, whose space-time evolution is decoupled from that of spectators [36, 54]. Consequently, they do not contribute to  $Cov(nA_{\text{sp}}, nA_{\text{ch},\eta})$ . However, these dynamics contribute to the fluctuations measured by  $Var(nA_{\text{sp}})$  in comparison to the scenario where they are absent. So, the existence of spectator dynamics is expected to decrease the magnitude of the proposed correlator. The reduction in  $\rho(nA_{\text{sp}}, nA_{\text{ch},\eta})$  caused by spectator dynamics, compared to its magnitude in the absence of such processes provides a strong constraint for modeling of spectator fragmentation and evaporation. Therefore, in addition to the sensitivity to preferential emission, the correlator  $\rho(nA_{\text{sp}}, nA_{\text{ch},\eta})$  also captures the effect of spectator dynamics.

**Results.** We first examine the impact of preferential emission on  $P(\eta)$  by categorizing events based on their initial-state asymmetry,  $A_{\text{sp}}$ , as shown in Figure 1(a). The events are divided into three categories: Region 1 for  $A_{\text{sp}} \ll 0$ , Region 2 for  $A_{\text{sp}} \gg 0$ , and Region 3 for  $A_{\text{sp}} \approx 0$ . Region 1 comprises events with a larger number of forward-going participants. According to preferential emission, particles from Region 1 are expected to predominantly populate large positive  $\eta$ , as seen in the  $P(\eta)$  distribution for these events in Figure 1(b). A comparison of  $P(\eta)$  ratios for events with  $A_{\text{sp}} \ll 0$  and  $A_{\text{sp}} \gg 0$  against those with

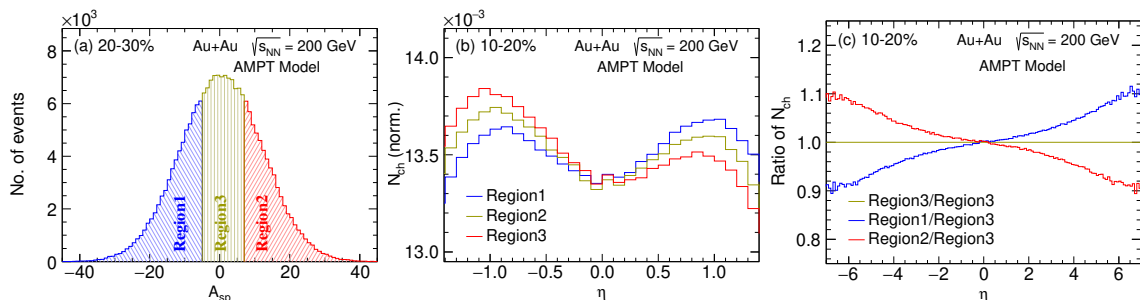


Figure 1: (a) Distribution of  $A_{\text{sp}}$  in 20–30% central Au+Au collisions at  $\sqrt{s_{\text{NN}}} = 200$  GeV. Regions 1, 2, and 3 denote events with  $A_{\text{sp}} \ll 0$ ,  $A_{\text{sp}} \gg 0$ , and  $A_{\text{sp}} \approx 0$ , respectively. (b) Comparison between  $\eta$  distribution of produced particles for events within Regions 1, 2, and 3. (c) Ratio between  $\eta$  distribution of produced particles for Region 1, Region 2, and Region 3 with respect to that of Region 3.

$A_{\text{sp}} \approx 0$ , shown in Figure 1(c), reveals an excess of produced particles in the forward or backward  $\eta$  for events with more forward or backward moving participants, respectively. Thus, Figure 1 confirms that particle production via string fragmentation in the AMPT model agrees with expectations from preferential emission.

The impact of preferential emission on particle production in forward/backward  $\eta$  is further quantified using the Pearson correlation as shown in Figure 2. First, we correlate  $N_{\text{spec},\text{F}}$  with  $N_{\text{ch},\eta}$  to obtain  $\rho(N_{\text{spec},\text{F}}, N_{\text{ch},\eta})$ . This correlator is observed to peak at forward  $\eta$ , indicating that the produced particles retain initial-state information about the direction of motion of participants, as expected from preferential emission [13]. The correlation between asymmetries in initial-state spectators and final-state multiplicities,  $\rho(nA_{\text{sp}}, nA_{\text{ch},\eta})$  is also shown in Figure 2. The rapidity-odd nature of  $\rho(nA_{\text{sp}}, nA_{\text{ch},\eta})$  is evident from the observation that,  $\rho(nA_{\text{sp}}, nA_{\text{ch},\eta}) = -\rho(nA_{\text{sp}}, nA_{\text{ch},-\eta})$ . As  $\eta \rightarrow 0$ ,  $(N_{\text{ch},\eta} - N_{\text{ch},-\eta}) \rightarrow 0$ , implying  $\rho(nA_{\text{sp}}, nA_{\text{ch},\eta}) \rightarrow 0$ .

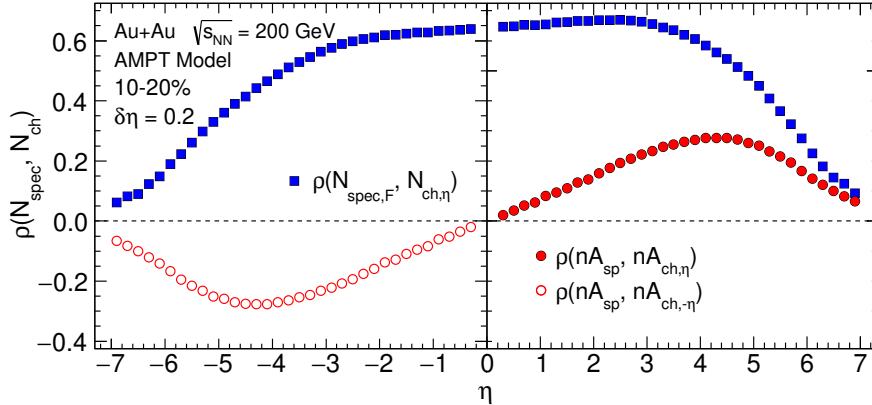


Figure 2:  $\rho(N_{\text{spec},F}, N_{\text{ch},\eta})$ ,  $\rho(nA_{\text{sp}}, nA_{\text{ch},\eta})$  and  $\rho(nA_{\text{sp}}, nA_{\text{ch},-\eta})$  for  $\delta\eta = 0.2$  in 20–30% central Au+Au collisions at  $\sqrt{s_{\text{NN}}} = 200$  GeV from the AMPT model.

The sensitivity of  $\rho(nA_{\text{sp}}, nA_{\text{ch},\eta})$  to variations in the number of particles falling within the  $\delta\eta$ -range is assessed by varying this range used for calculation of  $nA_{\text{ch},\eta}$ . The covariance and variances in the calculation of  $\rho(nA_{\text{sp}}, nA_{\text{ch},\eta})$  (Eq. 2) are found to be robust against statistical fluctuations arising from varying  $\delta\eta$  as shown in supplementary material.

Figure 3 shows  $\text{Var}(nA_{\text{ch},\eta})$ ,  $\text{Cov}(nA_{\text{sp}}, nA_{\text{ch},\eta})$ , and  $\rho(nA_{\text{sp}}, nA_{\text{ch},\eta})$  as a function of  $\eta$  for different centralities. The  $\text{Var}(nA_{\text{sp}})$  is depicted as horizontal lines near  $\eta = y_{\text{beam}}$  (beam rapidity,  $\approx 5.4$  for  $\sqrt{s_{\text{NN}}} = 200$  GeV [54]) because it is an initial-state quantity and does not change with  $\eta$  within the AMPT model simulation. The  $\text{Var}(nA_{\text{ch},\eta})$  gradually increases from mid- $\eta$  to  $y_{\text{beam}}$ , reflecting a growing forward-backward asymmetry in particle production as  $|\eta|$  increases driven by an increased fluctuations in string endpoints [23, 55].

The  $\text{Cov}(nA_{\text{sp}}, nA_{\text{ch},\eta})$  also shows an increasing trend with  $\eta$ , suggesting a stronger influence of initial-state asymmetry in  $N_{\text{part}}$  on the rapidity-odd components of  $P(\eta)$  with increasing  $|\eta|$ , consistent with findings in Refs. [11, 44]. The magnitude and shape of  $\rho(nA_{\text{sp}}, nA_{\text{ch},\eta})$  provides similar information as  $\text{Cov}(nA_{\text{sp}}, nA_{\text{ch},\eta})$ , but in a normalized form that removes contributions of the fluctuations in  $nA_{\text{ch},\eta}$  and  $nA_{\text{sp}}$ . The decrease in  $\rho(nA_{\text{sp}}, nA_{\text{ch},\eta})$  towards largest values of  $\eta$  arises because of a faster increase in  $\text{Var}(nA_{\text{ch},\eta})$  compared to  $\text{Cov}(nA_{\text{sp}}, nA_{\text{ch},\eta})$  in that region.

As collisions become increasingly central, the  $\text{Var}(nA_{\text{sp}})$  is observed to increase, which in turn, implies a decrease in  $\text{Var}(nA_{\text{part}})$ , following Eq. 3. The decrease in  $\text{Var}(nA_{\text{part}})$  indicates the formation of more equal numbers of strings from forward- and backward-moving participants as collisions become more central. On the other hand,  $\text{Var}(nA_{\text{ch},\eta})$  decreases as collisions become more central [11], suggesting more symmetric particle production about  $\eta=0$ , implying the formation of more longitudinally symmetric strings in central collisions.

$\text{Cov}(nA_{\text{sp}}, nA_{\text{ch},\eta})$  is shown in Figure 3(b) as a function of  $\eta$  for different centralities. The magnitude of the covariance only shows a small change with changing centrality. Interestingly,  $\rho(nA_{\text{sp}}, nA_{\text{ch},\eta})$ , shown in Figure 3(c), exhibits a clear centrality-dependent increase. This centrality dependence of  $\rho(nA_{\text{sp}}, nA_{\text{ch},\eta})$  mainly stems from  $\text{Var}(nA_{\text{sp}})$ , reflecting fluctuations in the number of strings, and  $\text{Var}(nA_{\text{ch},\eta})$ , reflecting the longitudinal asymmetry of the strings.

However, only spectator neutrons are typically measured in experiments by ZDC detectors [26, 27, 53]<sup>1</sup>. Therefore, to assess the sensitivity of the proposed correlator to spectator dynamics in a realistic experimental scenario, we compare the  $\rho(nA_{\text{sp}}, nA_{\text{ch},\eta})$  measured with (1) neutron spectators ( $n_{\text{spec}}$ ) from the AMPT model, which lacks spectator dynamics, and, (2) free-neutron spectators remaining after spectator dynamics detected by the ZDC referred to as “ $f_{\text{spec}}$ ” [54, 56]. The number of forward (backward) free-neutron

<sup>1</sup>In some experiments, both neutron and proton spectators can be measured[26]

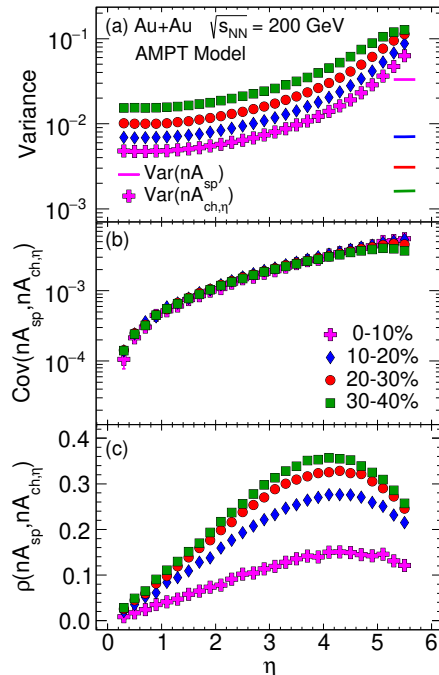


Figure 3: (a)  $Var(nA_{ch,\eta})$ , (b)  $Cov(nA_{sp}, nA_{ch,\eta})$ , and (c)  $\rho(nA_{sp}, nA_{ch,\eta})$  for different centralities as function of  $\eta$  in Au+Au collisions at  $\sqrt{s_{NN}} = 200$  GeV from the AMPT model.

spectators,  $f_{spec,F}$  ( $f_{spec,B}$ ) are estimated from experimental data using the method proposed in Ref. [11], briefly discussed here. The mean ( $\mu$ ) and width ( $\sigma$ ) of  $f_{spec}$  in Au+Au collisions at  $\sqrt{s_{NN}} = 200$  GeV were reported as functions of  $N_{part}$  in Ref. [54], based on the PHENIX data [56].

The number of spectators in forward and backward directions are independent of each other [28]. Therefore, to independently sample  $f_{spec,F}$  and  $f_{spec,B}$ , both  $\mu$  and  $N_{part}$  (shown in Figure A.6 of the supplementary material) were reduced by a factor of 2, and  $\sigma$  was scaled down by  $\sqrt{2}$  to obtain the correlation between  $f_{spec,F}$  and  $N_{part,F}$ . Then, for each value of  $N_{part,F}$  (or  $N_{part,B}$ ) obtained for each AMPT event, the  $f_{spec,F}$  (and  $f_{spec,B}$ ) is sampled from a Gaussian distribution with mean  $\mu_f = \mu/2$  and width  $\sigma_f = \sigma/\sqrt{2}$ . Finally, the proposed correlator, based on the estimated number of  $f_{spec,F}$  and  $f_{spec,B}$ , is calculated using Eq. 2.

Figure 4 shows the comparison of  $\rho(nA_{sp}, nA_{ch,\eta})$  calculated using the total spectators, neutron spectators, and free-neutron spectators (after they undergo spectator dynamics) from the AMPT model. To estimate sensitivity of varying spectator dynamics captured by  $Var(nA_{sp})$ , two cases with fluctuations of  $1\sigma_f$  and  $2\sigma_f$  are also shown. The magnitude of  $\rho(nA_{sp}, nA_{ch,\eta})$  using neutron spectators is smaller than those calculated with total spectators by a nearly constant factor of  $\sim 20\%$ , regardless of changing  $\eta$  or centrality (ratios in Figure A.7 in supplementary section). However, a strong centrality dependence of  $\rho(nA_{sp}, nA_{ch,\eta})$  for free-neutron spectators estimated from experimental data is observed. The  $\rho(nA_{sp}, nA_{ch,\eta})$  using free-neutron spectators in 0-10% central collisions is close to that of neutron spectators, whereas it is very close to zero for 30-40% centrality. Such a strong centrality dependence is expected from an increase in the spectator evaporation and fragmentation as increasingly more spectators become available for interaction as collision become more peripheral. This is consistent with GEMINI model simulations, which show that the effect of spectator dynamics on  $f_{spec}$  decreases as collisions become more central [57].

**Conclusion.** Understanding the longitudinal evolution of particle production is critical for constraining the three-dimensional shape of the medium formed in heavy-ion collisions. In various models, fragmentation of nucleons or strings in the initial state results in particles being preferentially emitted towards forward or backward pseudorapidities. Traditionally, the rapidity-odd component of the  $\eta$  profile is constrained using asymmetric collision systems within model scenarios. In contrast, this study proposes a Pearson correlation

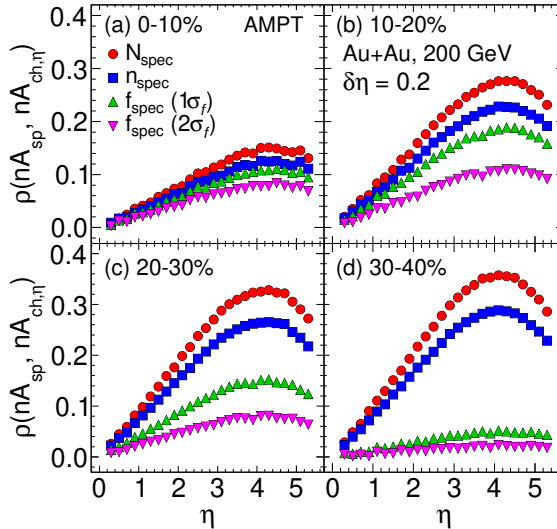


Figure 4: Comparisons between  $\rho(nA_{\text{sp}}, nA_{\text{ch}, \eta})$  calculated using total spectators and neutron spectators for  $\delta\eta = 0.2$  in Au+Au collisions at  $\sqrt{s_{\text{NN}}} = 200$  GeV from the AMPT model.

coefficient between the initial-state asymmetry of  $N_{\text{spec}}$  and the  $\eta$ -asymmetry of  $N_{\text{ch}}$  in experimental collision of symmetric systems to quantify the role of preferential emission towards the rapidity-odd component of pseudorapidity distribution of particles.

The results reveal that the final-state longitudinal asymmetry in produced particles is strongly correlated with the initial-state asymmetry between forward- and backward-moving participants with the magnitude increasing from mid- $\eta$  to forward  $\eta$ , as expected from preferential emission mechanism. Additionally, for central collisions, a smaller correlator magnitude is observed, attributable to reduced forward-backward participant asymmetry and the formation of more longitudinally symmetric strings. Using the AMPT model, we demonstrate the feasibility of this measurement in heavy-ion collision experiments.

A unique aspect of the proposed correlator is that it assumes only an inherent categorization of nature of particle production sources into rapidity-odd and rapidity-even components, without making explicit assumptions about the particle production process itself. The observed rapidity-odd behavior emerges naturally from the particle production mechanism implemented within the model. Therefore, an experimental measurement of this correlator can provide a crucial test for the influence of preferential emission on both particle distribution and phenomena such as flow-decorrelations and directed-flow.

Using experimental data from PHENIX, we show that the proposed correlator is highly sensitive to processes governing spectator matter evolution. Increased fluctuations in the number of spectators, due to evaporation and fragmentation, reduce the correlator's magnitude. At lower collision energies, spectator dynamics have been reported to influence the  $\eta$  distribution of charged particles closer to  $\eta = 0$  than at higher energies [56]. Therefore, the proposed correlator could be used to constrain these contribution at lower energies.

Thus, the novel observable,  $\rho(nA_{\text{sp}}, nA_{\text{ch}, \eta})$  offers a valuable handle to constrain the mechanisms governing pseudorapidity distribution of produced particles as well as space-time evolution of spectators in heavy-ion collisions. Future measurements of this correlator across different collision energies, particularly in the beam energy scan at RHIC, FAIR, and NICA experimental facilities would help understand the energy dependence of spectator interactions and the nuclear EoS.

**Acknowledgements.** The authors thank Subhasish Chattopadhyay, Govert Nijs, Victor Roy, Subhash Singha and Chunjian Zhang for their valuable comments. We also thank Elena Bratkovskaya for her insightful suggestions. SB is supported by U.S Department of Energy under grant number DEFG0287ER40331.

## References

- [1] M. Li and C. Shen, *Phys. Rev. C* **98**, 064908 (2018), arXiv:1809.04034 [nucl-th] .
- [2] G. S. Denicol *et al.*, *Phys. Rev. C* **98**, 034916 (2018), arXiv:1804.10557 [nucl-th] .
- [3] L. Du *et al.*, *Phys. Rev. C* **104**, 064904 (2021), arXiv:2107.02302 [hep-ph] .
- [4] C. Shen and B. Schenke, *Phys. Rev. C* **105**, 064905 (2022), arXiv:2203.04685 [nucl-th] .
- [5] C. Shen and S. Alzhrani, *Phys. Rev. C* **102**, 014909 (2020), arXiv:2003.05852 [nucl-th] .
- [6] L. Du *et al.*, *Phys. Rev. C* **108**, L041901 (2023), arXiv:2211.16408 [nucl-th] .
- [7] J. Jia and P. Huo, *Phys. Rev. C* **90**, 034905 (2014), arXiv:1402.6680 [nucl-th] .
- [8] J. Jia *et al.*, *J. Phys. G* **44**, 075106 (2017), arXiv:1701.02183 [nucl-th] .
- [9] M. Aaboud *et al.* (ATLAS Collaboration), *Eur. Phys. J. C* **78**, 142 (2018), arXiv:1709.02301 [nucl-ex] .
- [10] G. Aad *et al.* (ATLAS Collaboration), *Phys. Rev. Lett.* **126**, 122301 (2021), arXiv:2001.04201 [nucl-ex] .
- [11] J. Jia *et al.*, *Phys. Rev. C* **93**, 044905 (2016), arXiv:1506.03496 [nucl-th] .
- [12] G. Aad *et al.* (ATLAS Collaboration), *JHEP* **07**, 019 (2012), arXiv:1203.3100 [hep-ex] .
- [13] M. Gazdzicki and M. I. Gorenstein, *Phys. Lett. B* **640**, 155 (2006), arXiv:hep-ph/0511058 .
- [14] M. Gyulassy and X.-N. Wang, *Comput. Phys. Commun.* **83**, 307 (1994), arXiv:nucl-th/9502021 .
- [15] Z.-W. Lin *et al.*, *Phys. Rev. C* **72**, 064901 (2005), arXiv:nucl-th/0411110 .
- [16] S. Ferreres-Solé and T. Sjöstrand, *Eur. Phys. J. C* **78**, 983 (2018), arXiv:1808.04619 [hep-ph] .
- [17] M. Rohrmoser and W. Broniowski, *Phys. Rev. C* **99**, 024904 (2019), arXiv:1809.08666 [nucl-th] .
- [18] W. Broniowski and M. Rohrmoser, *Acta Phys. Polon. B* **50**, 1019 (2019), arXiv:1904.06955 [nucl-th] .
- [19] A. Bialas and W. Czyz, *Acta Phys. Polon. B* **36**, 905 (2005), arXiv:hep-ph/0410265 .
- [20] A. Bzdak, *Phys. Rev. C* **80**, 024906 (2009), arXiv:0902.2639 [hep-ph] .
- [21] A. Bzdak and K. Wozniak, *Phys. Rev. C* **81**, 034908 (2010), arXiv:0911.4696 [hep-ph] .
- [22] P. Bozek and I. Wyskiel, *Phys. Rev. C* **81**, 054902 (2010), arXiv:1002.4999 [nucl-th] .
- [23] P. Bozek and W. Broniowski, *Phys. Lett. B* **752**, 206 (2016), arXiv:1506.02817 [nucl-th] .
- [24] L.-G. Pang *et al.*, *Eur. Phys. J. A* **52**, 97 (2016), arXiv:1511.04131 [nucl-th] .
- [25] M. Rohrmoser and W. Broniowski, *Phys. Rev. C* **101**, 014907 (2020), arXiv:1909.01702 [nucl-th] .
- [26] G. Dellacasa *et al.* (ALICE Collaboration), CERN-LHCC-99-05 (1999), <https://cds.cern.ch/record/381433> .
- [27] R. Arnaldi *et al.*, *Nucl. Instrum. Meth. A* **581**, 397 (2007), [Erratum: *Nucl. Instrum. Meth. A* 604, 765 (2009)] .
- [28] R. Staszewski *et al.*, *Acta Phys. Polon. B* **50**, 1229 (2019), arXiv:1903.09498 [physics.ins-det] .
- [29] J. J. Chwastowski *et al.*, (2020), arXiv:2011.00872 [hep-ex] .
- [30] J. J. Gaimard and K. H. Schmidt, *Nucl. Phys. A* **531**, 709 (1991).
- [31] J. Hufner *et al.*, *Phys. Rev. C* **12**, 1888 (1975).
- [32] A. Sorensen *et al.*, *Prog. Part. Nucl. Phys.* **134**, 104080 (2024), arXiv:2301.13253 [nucl-th] .
- [33] L. Zheng, E. C. Aschenauer, and J. H. Lee, *Eur. Phys. J. A* **50**, 189 (2014), arXiv:1407.8055 [hep-ex] .
- [34] L. Shi, *Transport phenomena in heavy-ion reactions*, Ph.D. thesis, Michigan State U. (2003).
- [35] N. Collaboration (NA49), *Eur. Phys. J. A* **2**, 383 (1998).
- [36] B. B. Back *et al.* (PHOBOS Collaboration), *Phys. Rev. C* **94**, 024903 (2016), arXiv:1511.07921 [nucl-ex] .
- [37] L. Adamczyk *et al.* (STAR), *Phys. Rev. Lett.* **112**, 162301 (2014), arXiv:1401.3043 [nucl-ex] .
- [38] M. Nie (STAR), *Nucl. Phys. A* **1005**, 121783 (2021), arXiv:2005.03252 [nucl-ex] .
- [39] P. Bozek *et al.*, *Phys. Rev. C* **83**, 034911 (2011), arXiv:1011.3354 [nucl-th] .
- [40] W. Broniowski and P. Bozek, *EPJ Web Conf.* **141**, 05003 (2017), arXiv:1610.09673 [nucl-th] .
- [41] A. Bialas and A. Bzdak, *Phys. Rev. C* **77**, 034908 (2008), arXiv:0707.3720 [hep-ph] .
- [42] A. Bzdak, *Acta Phys. Polon. B* **41**, 151 (2010), arXiv:0904.0869 [hep-ph] .
- [43] B. Kellers and G. Wolschin, *PTEP* **2019**, 053D03 (2019), arXiv:1901.06421 [hep-ph] .
- [44] J. Jia (ATLAS Collaboration), *Nucl. Phys. A* **956**, 405 (2016), arXiv:1601.01296 [nucl-ex] .
- [45] J. Jia *et al.*, *Phys. Rev. Lett.* **131**, 022301 (2023), arXiv:2206.10449 [nucl-th] .
- [46] J. Xu and C. M. Ko, *Phys. Rev. C* **84**, 044907 (2011), arXiv:1108.0717 [nucl-th] .
- [47] J. Xu and C. M. Ko, *Phys. Rev. C* **84**, 014903 (2011), arXiv:1103.5187 [nucl-th] .
- [48] D. Solanki *et al.*, *Phys. Lett. B* **720**, 352 (2013), arXiv:1210.0512 [nucl-ex] .
- [49] J. Jia *et al.*, *Chin. Phys. Lett.* **40**, 042501 (2023), arXiv:2206.07184 [nucl-th] .
- [50] E. G. Nielsen and Y. Zhou, *Eur. Phys. J. C* **83**, 545 (2023), arXiv:2211.13651 [nucl-ex] .
- [51] N. Magdy *et al.*, *Universe* **6**, 146 (2020), arXiv:2009.02734 [nucl-ex] .
- [52] Z.-W. Lin and L. Zheng, *Nucl. Sci. Tech.* **32**, 113 (2021), arXiv:2110.02989 [nucl-th] .
- [53] Y.-F. Xu *et al.*, *Nucl. Sci. Tech.* **27**, 126 (2016).
- [54] S. Tarafdar *et al.*, *Nucl. Instrum. Meth. A* **768**, 170 (2014), arXiv:1405.4555 [nucl-ex] .
- [55] X.-Y. Wu, L.-G. Pang, G.-Y. Qin, and X.-N. Wang, *Phys. Rev. C* **98**, 024913 (2018), arXiv:1805.03762 [nucl-th] .
- [56] PHENIX Collaboration (PHENIX), *Phys. Rev. C* **71**, 034908 (2005), [Erratum: *Phys. Rev. C* 71, 049901 (2005)], arXiv:nucl-ex/0409015 .
- [57] L.-M. Liu, C.-J. Zhang, J. Zhou, J. Xu, J. Jia, and G.-X. Peng, *Phys. Lett. B* **834**, 137441 (2022), arXiv:2203.09924 [nucl-th] .

## Appendix A.

One of the main physics objectives of the proposed correlator,  $\rho(nA_{\text{sp}}, nA_{\text{ch},\eta})$ , is to investigate the relationship between the initial state asymmetry in the number of forward and backward-going spectators,  $nA_{\text{sp}}$ , and the forward-backward asymmetry in multiplicity,  $nA_{\text{ch},\eta}$ , in the final state. The number of charged particles within a given  $\eta$ -interval,  $\delta\eta$ , fluctuates on an event-by-event basis. Therefore, it is essential to examine the sensitivity of the proposed correlator to the size of  $\delta\eta$ . Figure A.5 shows  $\text{Var}(nA_{\text{ch},\eta})$ ,  $\text{Cov}(nA_{\text{sp}}, nA_{\text{ch},\eta})$ , and  $\rho(nA_{\text{sp}}, nA_{\text{ch},\eta})$  for different values of  $\delta\eta$ . The variance, covariance, and the correlator remains unaffected by variations in  $\delta\eta$  window.

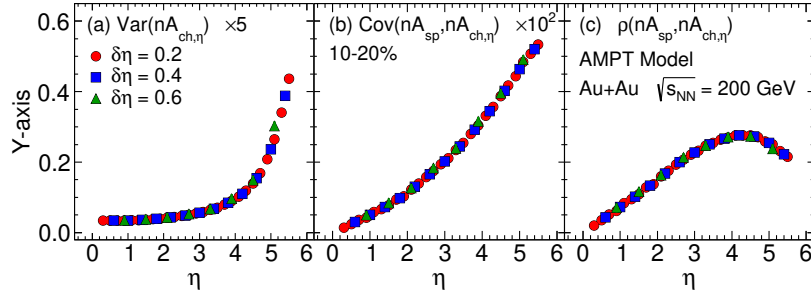


Figure A.5: (a)  $\text{Var}(nA_{\text{ch},\eta})$ , (b)  $\text{Cov}(nA_{\text{sp}}, nA_{\text{ch},\eta})$ , and (c)  $\rho(nA_{\text{sp}}, nA_{\text{ch},\eta})$  as a function of  $\eta$  for different  $\delta\eta$  in 20–30% central Au+Au collisions at  $\sqrt{s_{\text{NN}}} = 200$  GeV. The  $\text{Var}(nA_{\text{ch},\eta})$  and  $\text{Cov}(nA_{\text{sp}}, nA_{\text{ch},\eta})$  are arbitrarily scaled for better visibility.

Figure A.6(a) shows the estimated number of free-neutrons detected by the ZDC from the PHENIX experiment at RHIC versus the total number of participants. The 2D correlation is constructed using  $\mu$  and  $\sigma$  from the PHENIX data for Au+Au collisions at  $\sqrt{s_{\text{NN}}} = 200$  GeV [56], as reported in Ref. [54]. The number of forward-going spectators versus forward participants is then estimated from the correlation in panel (a), following the methodology proposed in Ref. [11], and briefly discussed in the paper, as shown in panel (b) of Figure A.6.

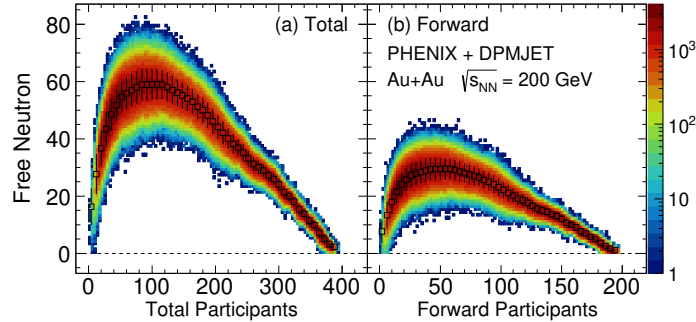


Figure A.6: (a)  $f_{\text{spec}}$  vs  $N_{\text{part}}$  for Au+Au collisions at  $\sqrt{s_{\text{NN}}} = 200$  GeV simulated using estimated mean and sigma of  $f_{\text{spec}}$  at given  $N_{\text{part}}$  in Ref. [54] using PHENIX data [56]. (b)  $f_{\text{spec},\text{F}}$  vs  $N_{\text{part},\text{F}}$  estimated using panel (a) following the methodology described in text. The respective mean and sigma values used are shown in black points and lines, respectively.

Figure A.7 illustrates the impact of spectator dynamics on the proposed correlator. To demonstrate this, the ratio of  $\rho(nA_{\text{sp}}, nA_{\text{ch},\eta})$  measured using total spectators ( $N_{\text{spec}}$ ) and free-neutron spectators ( $f_{\text{spec}}$ , after accounting for spectator dynamics) is shown relative to the neutron spectators ( $n_{\text{spec}}$ ) from AMPT across four different centralities. The sensitivity to varying spectator dynamics is evaluated by adjusting  $\sigma_f$ . It is evident that  $\rho(nA_{\text{sp}}, nA_{\text{ch},\eta})$  calculated using  $n_{\text{spec}}$  is consistently smaller than those calculated with  $N_{\text{spec}}$  by approximately 20%, regardless of centrality or  $\eta$ . However, after spectator dynamics, a significant decrease is observed with increasing  $\sigma_f$ , especially for relatively peripheral centralities.



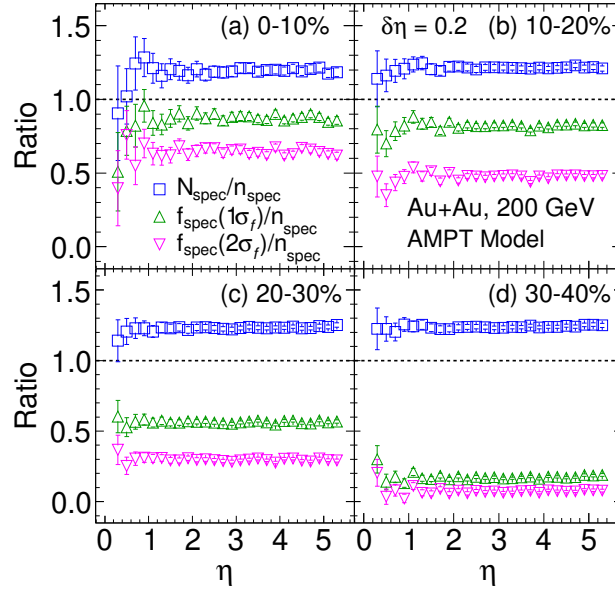


Figure A.7: Ratio between  $\rho(nA_{\text{sp}}, nA_{\text{ch}, \eta})$  calculated using total spectators ( $N_{\text{spec}}$ ) and free-neutron spectators ( $f_{\text{spec}}$ ) in comparison to that calculated with neutron spectators ( $n_{\text{spec}}$ ) for  $\delta\eta = 0.2$  in Au+Au collisions at  $\sqrt{s_{\text{NN}}} = 200$  GeV. The  $1\sigma_f$  and  $2\sigma_f$  refer to two considered cases for different amount of fluctuations in  $f_{\text{spec}}$  owing to spectator dynamics.